Design and operation of LongBo: a 2 m long drift liquid argon TPC

M. Adamowski[a], B. Carls[a], E. Dvorak[b], A. Hahn[a], W. Jaskierny[a], C. Johnson[c], H. Jostlein[a], C. Kendziora[a], S. Lockwitz[a], B. Pahlka[a], R. Plunkett[a], S. Pordes[a], B. Rebel[a], R. Schmitt[a], M. Stancari[a], T. Tope[a] and T. Yang[a]

[a] *Fermi National Accelerator Laboratory, P.O. Box 500, Batavia, IL, 60510, USA*
[b] *South Dakota School of Mines & Technology, 501 East Saint Joseph Street, Rapid City, SD 57701, USA*
[c] *Indiana University, 727 E. Third St., Swain Hall West, Room 117, Bloomington, IN 47405, USA*

ABSTRACT: In this paper, we report on the design and operation of the LongBo time projection chamber in the Liquid Argon Purity Demonstrator cryostat. This chamber features a 2 m long drift distance. We achieved high liquid argon purity with the chamber inside the cryostat.

KEYWORDS: LArTPC.

Contents

1. Introduction

The liquid argon (LAr) time projection chambers (TPCs) provide excellent spatial and calorimetric resolutions for measuring the properties of neutrino interactions above a few MeV. Conventional liquid argon vessels are evacuated to remove water, oxygen and nitrogen contaminants present in the ambient air prior to filling with liquid argon. However, as physics requirements dictate larger cryogenic vessels to hold bigger detectors, the mechanical strength required to resist the external pressure of evacuation becomes prohibitively costly. The Liquid Argon Purity Demonstrator (LAPD) [1] was an R&D test stand at Fermilab designed to determine if electron drift lifetimes adequate for large neutrino detectors could be achieved without first evacuating the cryostat. The electron drift lifetime in this test measured with purity monitors was greater than 6 ms without initial evacuation of the cryostat, which largely exceeds the required electron drift lifetime for the future large LArTPCs.

After achieving the required electron drift lifetimes, the LAPD cryostat was emptied and a TPC of 2 m drift distance, the LongBo TPC, was installed in the central cryostat region. High liquid argon purity was achieved with the TPC in the tank. This paper summarizes the design and operation of the LongBo TPC, which for the first time achieved a drift distance of 2 m in the US LArTPC programs.

2. Construction of the "Long Bo" TPC

The "Long Bo" TPC that operated in the LAPD Cryostat had a sensitive volume of 25 cm diameter by 2 m long. We will describe here its design and how it was made.

The Long Bo TPC is an extended-length version of the "Bo" TPC that was made a few years earlier. The Bo TPC had an active volume of 25 cm diameter by 50 cm long. It had three sense wire planes, with wires oriented at 60 degrees from each other. The wires were 4.7 mm spaced and were 125 micron diameter beryllium copper. They were hand-soldered to a 3 mm thick copper-clad G10 board for each plane. The copper cladding was routed in a pad pattern on a Fermilab CNC router. Wire connections were also hand-soldered to the wire pads and routed to connectors, from which Olefin insulated flat cables took the signals to the cold pre-amplifiers. The planes were biased from external voltage sources via a feed through. Fig. 1 shows the wire planes and the cold pre-amplifiers that amplify the wire signals. The cathode was made from copper mesh, chosen to allow free argon flow along the TPC axis. The mesh was stretched inside a ring made of 19 mm diameter stainless steel tube. A stainless steel tube elbow was welded to this ring and served to connect to the high voltage feed through, described in Section 3, via a cup and spring-finger connection.

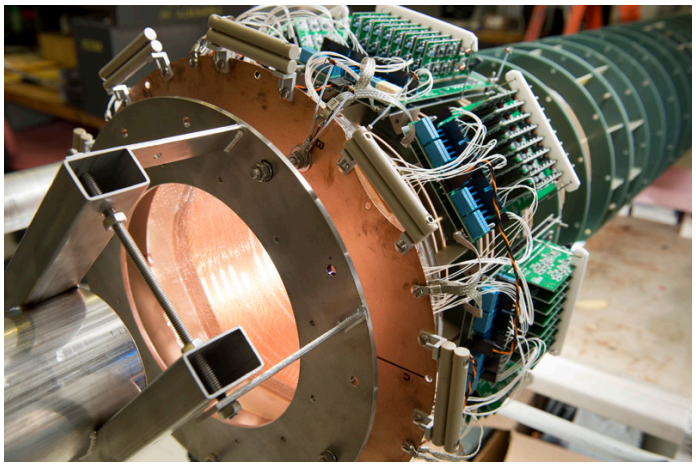

Figure 1: The wire planes and cold pre-amplifiers.

A uniform electric drift field was provided by a cylinder made of a copper-clad, 0.6 mm thick, G10 sheet, which is 50 cm long by 78 cm wide. The sheet was routed to provide 18 mm wide copper strips, separated by 1.5 mm wide spaces. The sheet was rolled into a 25 cm diameter tube which was inserted into a set of 7 rings routed from 4 mm thick G10. The left-over discs were mounted on a 13 mm threaded rod which was used to impose the required cylindrical shape as the sheets were epoxied to the inner surface of the rings. Two strings, for redundancy, of 100 MOhm voltage divider resistors, Ohmite model 104, rated at 10 kV, 1 W, were soldered to the inner surface of the copper sheet. Fig. 2 shows the resistors soldered to the inner surface of the copper sheet.

"Bo" was converted to "Long Bo" by inserting three additional drift field sections, each 50 cm long, for a total drift length of 2 m. Ribs were added to strengthen the first and last ring connection to the cylinder. The rings had screw holes to connect them to each other to make the 2 m long

Figure 2: The resistors soldered to the inner surface of the copper sheet.

assembly. beryllium copper spring stock were soldered to the ends of each cylinder to assure interconnection at the joints.

The TPC was supported by bolting a 3 mm thick stainless steel ring to the cathode end. The ring was connected to an articulating joint to facilitate installation in the low-overhead space on top of the LAPD cryostat. Fig. 3 shows the assembled TPC with high voltage feedthrough and electronics.

3. The High Voltage System

To provide the electric field to drift the signal electrons, a high voltage was applied to the cathode mesh on the bottom of the TPC. The high voltage system consisted of a power supply, a filter pot, and a feedthrough.

The high voltage was generated outside of the cryostat by a Glassman LX150N12 power supply [3]. The supply was controlled remotely by a program and was set to trip if more than 1.1 mA of current was drawn.

Before entering the cryostat, the voltage was passed through a filter pot. This low-pass filter was a sealed aluminum vessel with cable receptacles that electrically connected to eight 10 MΩ resistors submerged in Diala oil. The capacitance for the filter was supplied by the cable to the feedthrough. The purpose of the pot was twofold: it reduced the high-frequency ripple from the power supply, and it would limit the energy to the TPC in the case of a high voltage discharge.

The feedthrough transmits the high voltage into the cryostat and to the receptacle cup of the cathode plane. This feedthrough is shown in Fig 4 and was modeled after the feedthrough used in the ICARUS experiment with a stainless steel inner conductor insulated radially by ultra high molecular weight polyethylene (UHMW PE), and surrounded by a stainless steel ground tube. Grooves were added to the exposed UHMW PE to reduce surface currents. Initially, conducting shielding cups, shown in Fig 4b, were installed to reduce the field along the feedthrough. Midway

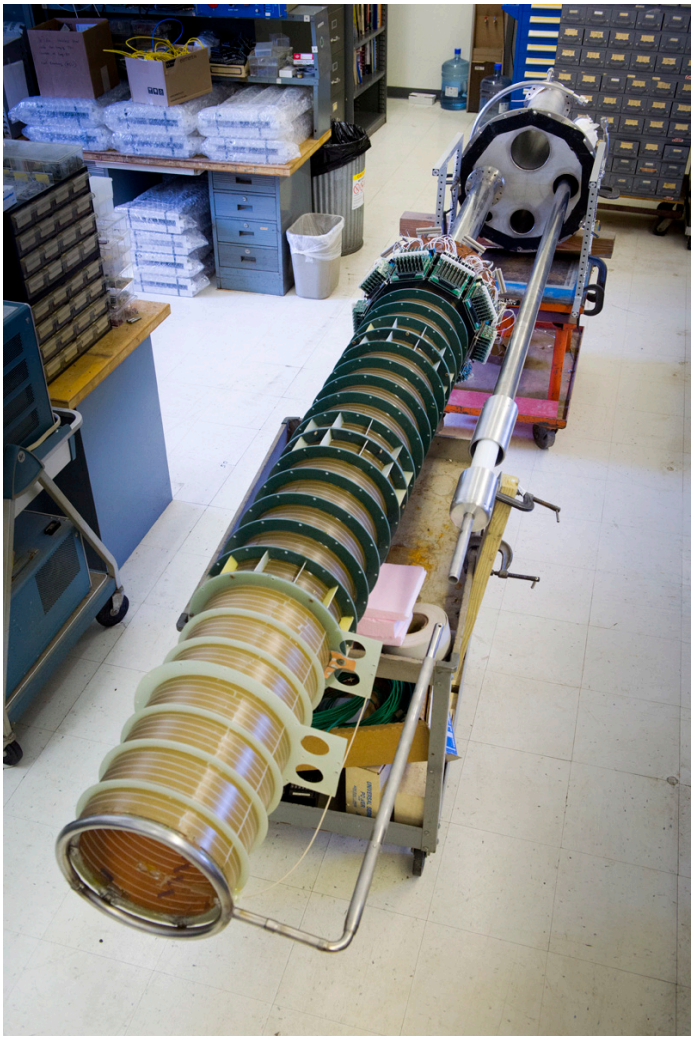

Figure 3: Assembled LongBo TPC.

through running, the cups were removed to determine what effect they had on performance. No change was seen. To ensure good electrical contact, the feedthrough has a spring tip that is inserted into a receptacle cup attached to the cathode plane.

4. Electronics

The LArTPC technology was pioneered by the ICARUS collaboration using warm electronics with a dual-jFET charge integrating front-end preamp. For each wire of the detector the feed-through passed DC bias-voltage into the cryostat and passed the TPC signals back to the electronics. Early development in the US used a similar warm preamplifier on a 3-plane LArTPC detector (Bo) built by Fermilab with wires on a 4.6 mm pitch, and used a 32-channel ADF2 digitizer built by MSU for the D0 experiment. At the same time the ArgoNeuT LArTPC was built and used the same warm preamplifier design readout with the ADF2 at 5 MHz, however, the DC bias-voltage distribution

(a)

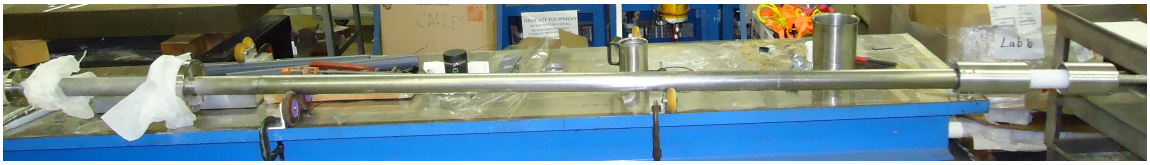

(b)

Figure 4: Photographs of the HV feedthrough without (a) and with (b) the electric field shielding cups.

to each wire and its signal-decoupling capacitor were mounted on the TPC in the liquid Ar. This allowed the feed-through to use high-density connectors for wire signals alone. The 480-channels of warm preamplifier for the 4-mm wire pitch (at 60Âř to the beam) of the ArgoNeuT LArTPC, exhibited a noise of 1.4 ADC-counts and a collection plane signal (attenuation-corrected) of 32 ADC-counts for 4.6 mm samples along minimum-ionizing muon tracks. During 2009-10 the ArgoNeuT detector recorded 10,000 neutrino interactions, underground in the NuMI beam at Fermilab.

The development of cold electronics for a LArTPC was driven by fact that at the 87K temperature of LAr there is less intrinsic noise in a MOSFET preamp than in the best warm preamp, and by mounting the preamp on the TPC the noise generated by a cable capacitance can be eliminated. While ArgoNeuT was running, a cold MOSFET preamp-filter card was designed and 144 channels were built and deployed on the Bo LArTPC and digitized by the ADF2. In this first application of a MOSFET front-end on a LArTPC, the preamp-filter was implemented with a 2.1 Âţsec "peaking time". For samples with an effective length of 4.6 mm on minimum ionizing muon tracks, the preamp-filter exhibited a signal-to-noise ratio of about 30, approximately 25% better than the warm preamplifiers discussed above. A similar performance for these amplifiers was measured when these "discrete" MOSFET preamp-filter cards were used on the long-Bo LArTPC described in this paper. For this data, the ADF2 FPGA was reprogrammed to digitize 16-channels at 2 MHz.

A MOSFET ASIC preamp-filter for use at cryogenic temperatures was designed by BNL for the MicroBoone experiment. Also, it is a candidate for readout of the LArTPC detectors for LBNE. A version (V4) of this 16-channel ASIC became available in 2012 and could be implemented for 2013 run of the long-Bo LArTPC. One 16-channel preamp-filter card was modified to use a section of the MicroBoone motherboard that serviced a single ASIC as a mezzanine board. The input/output connectors, bias-voltage distribution and decoupling capacitors of the card were retained. An ASIC control box was built which could set the gain and peaking time parameters of the ASIC. The ASIC modified preamp-filter card was installed in place of one induction plane card with the signals processed by the same digitizing electronics. Using a 2 Âţsec peaking time for the filter, the ASIC signal to noise was about 42, or 40% better than the "discrete" preamp-filter, and

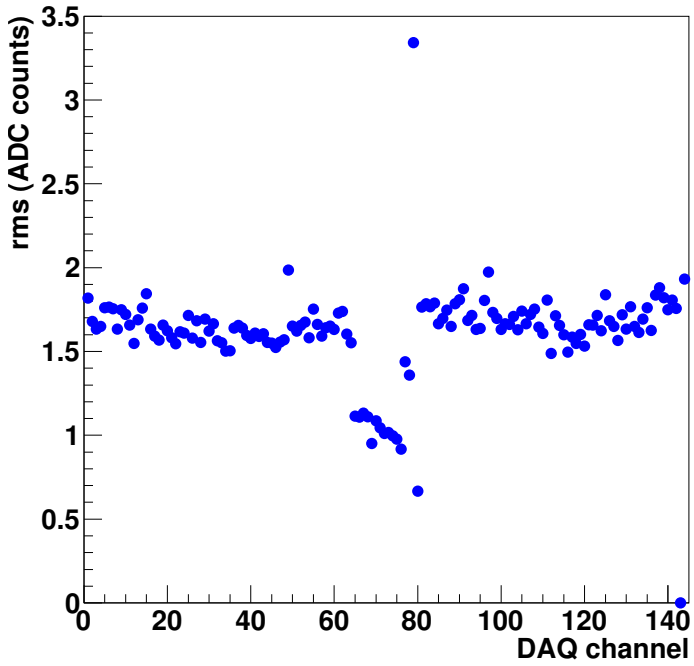

Figure 5

about 75% better than observed for readout with a warm preamplifier. The impressive performance of the BNL ASIC bodes well for its use in experiments at Fermilab and elsewhere.

5. Signal to Noise Ratio

To measure the noise for each channel, a special run of 200 events was taken with a random trigger and no drift field. For each channel, the measured ADC counts for all 200 events were combined and the distribution fit to a Gaussian function. The width of the best fit Gaussian is reported as the noise in figure 5.

The signal strength was extracted from straight muon tracks. To measure the S/N ratio of the discrete CMOS electronics chain, good tracks were selected by hand with the event display, whose projection onto the collection plane wires was nearly perpendicular to wire direction and centered on the wire plane. The pulse height of the signal on each wire is recorded as the maximum ADC count in the waveform. Of the wires in the collection plane with signals from the track, the outermost two on either side of the wire plane were excluded from the analysis as a fiducial volume cut intended to reject hits close to the field cage where uniformity is questionable and the pulse heights are noticeably reduced. In addition, wires with pulse heights greater than 1.5 times the average pulse height were excluded.

In the absence of diffusion, the length of track which contributes to the signal on a particular collection plane wire is $\frac{\Delta w}{\sin(\theta)\cos(\phi)}$, where $\Delta w = 4.7$ mm is the wire spacing and θ and ϕ are the reconstructed track angles defined in section 2 of the draft. The individual measured pulse heights were reduced by a factor of $\sin(\theta)\cos(\phi - 60^o)$ before taking the average of all *good* collection

	$S/S_{discrete}$	N	$(S/N)/(S/N)_{discrete}$
discrete	50.26/50.26	1.69	1
ASIC - 0.5 μs	10.1/36.0	0.55	0.9
ASIC - 1.0 μs	19.3/36.0	0.75	1.2
ASIC - 2.0 μs	33.6/36.0	1.10	1.4
ASIC - 3.0 μs	40.3/36.0	1.35	1.4

Table 1: All values are in ADC counts except the unitless ratios.

wire values from the 10-12 event sample to obtain the value of S reported in table 1 for the discrete electronics chain.

The 16 ASIC channels were connected to the center 16 wires of the middle (induction) wire plane. For these bi-polar signals, the signal height was recorded as the minimum ADC count of the waveform. Tracks whose projection onto the middle wire plane is perpendicular to the wire direction were selected ($\phi \sim 60^o$) and the extracted pulse heights were normalized by the factor $\sin(\theta)\cos(\phi - 60^o)$. The ratio of the average pulse height for ASIC and discrete channels is reported in table 1 for different values of the shaping time constant.

To investigate the effect of the shaping time constant on the pulse shape, the signal from wire 67 for one event for each shaping time is plotted in figure 6. The signals are scaled to have the same peak height to facilitate comparison. The small differences in shape could be due to slightly different drift times and or track angles.

6. Trigger

The presence of a through-going muon was detected by three sets of scintillation counters placed around the exterior of the LAPD tank. Each set consisted of two groups of counters placed on opposite sides of the tank, with the line intersecting the groups of counters passing roughly perpendicular to the wire direction for one wire plane. Each group consisted of four counters, stacked in a column for an effective area of scintillator roughly 8 feet by 2 feet. A coincidence was required between counters on opposite side of the tanks, and the track angle coverage is shown in section 8.

7. Operation

The LongBo TPC was inserted into the LAPD cryostat together with the high voltage feed through on October 25, 2012. Fig. 7 shows the positions of the TPC and the high voltage feed through inside the LAPD tank.

The gaseous argon piston purge was started on December 29, 2012. The argon gas recirculation was started on December 30, 2012. The cryostat was filled with liquid argon on January 10, 2013. The details of those filtration steps are documented in [1]. The high voltage was raised on January 25, 2013. The TPC data taking started since then until September 2013. Most of the data were taken during the evenings and weekends to avoid noised induced by welding work in the pit during work days.

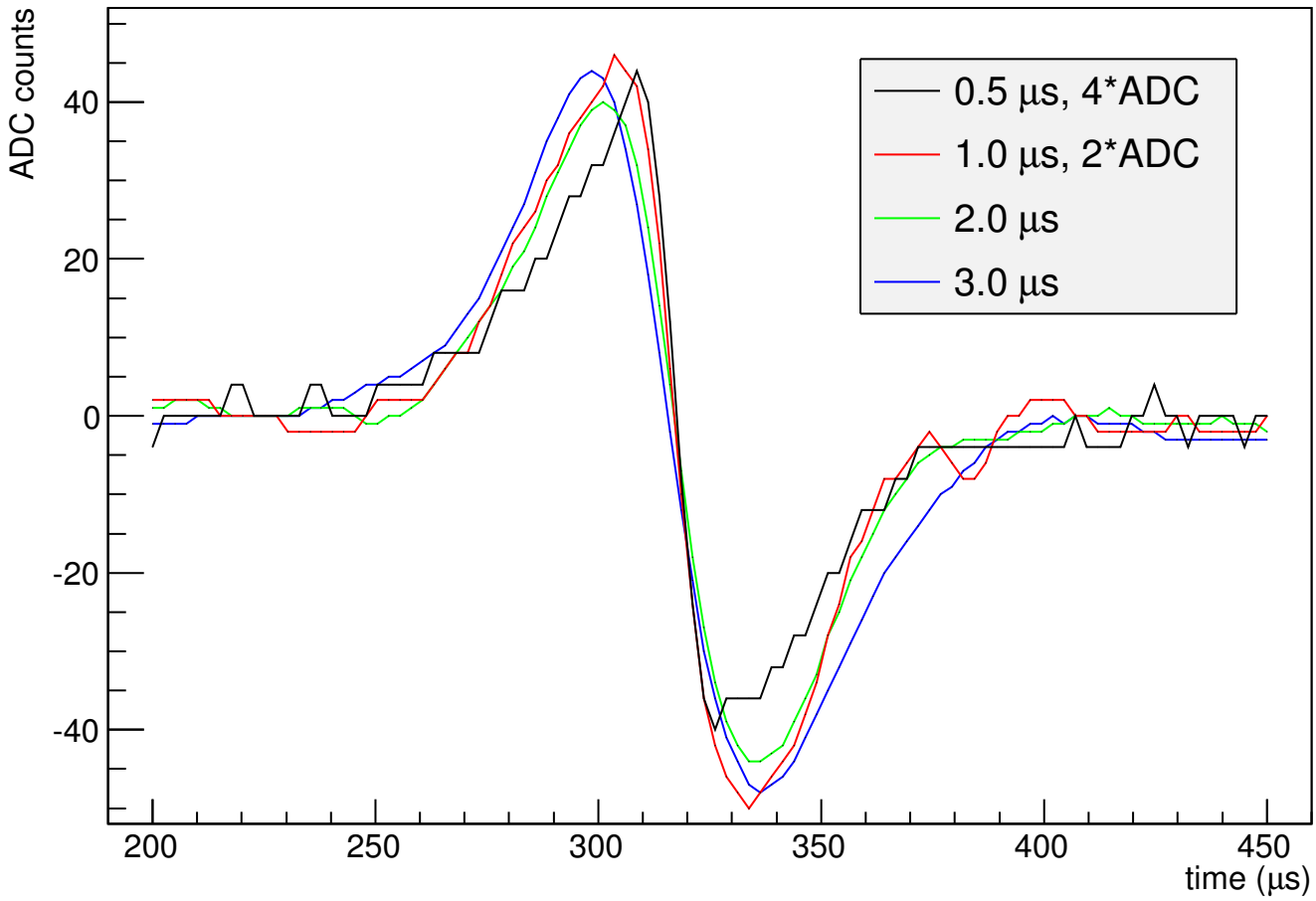

Figure 6: The horizontal axis has an arbitrary zero so that the pulses are shown with the zero crossing point roughly aligned artifically. The tracks from which these signals are taken form an angle of roughly 20 degrees with the plane of the wires $\theta \sim 70$. The angle between the projection of the track onto the wire plane and the wires themselves is ~ 80 degrees.

An issue we had in the LongBo run was that the high voltage tripped off numerous times due to sparking the first time we tried to raise high voltage. This forced the running of a low high voltage, ultimately reaching a maximum 75 kV, with occasional trips, instead of the nominal 100 kV for a 2 m drift TPC. The reason for the high voltage breakdown is unclear and being investigated. Even with the lower-than-nominal high voltage, we recorded several hundred thousand clear cosmic ray muon tracks in our data, which were used to study the electronics performance and liquid argon purity.

8. Measurment of Electron Attenuation Using Cosmic Ray Muons

When cosmic ray muons pass through the liquid argon, they deposit energy through ionization. The

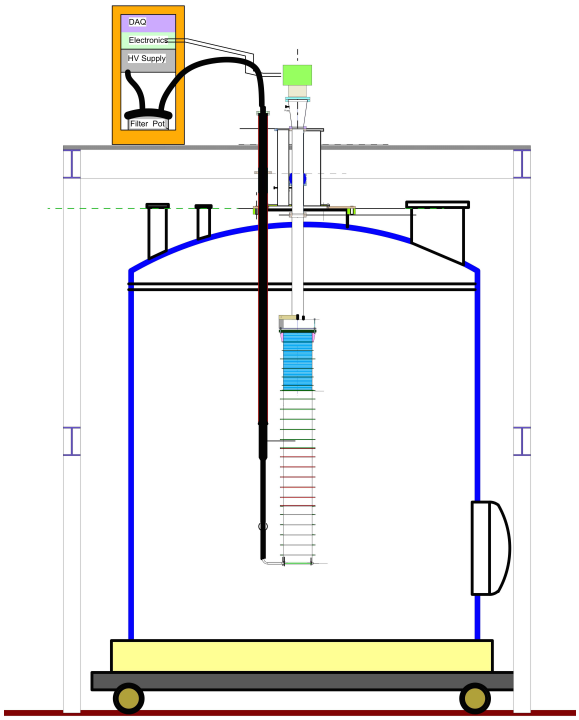

Figure 7: The TPC and high voltage feed through inside the LAPD tank.

ionization electrons are drifted by the electric field and collected by the wire planes. The variation of the energy deposition along the muon track is small for the energetic muons. By examining the signal recorded by each wire as a function of electron drift time, one can measure the attenuation of ionization electrons along the drift distance and determine the electron lifetime. This method was used by ArgoNeuT to derive the electron lifetime [2].

We analyzed cosmic ray muon data taken between April 8 and June 21. This corresponds to a full cycle of LAPD running, from liquid pump start to pump end. The high voltage we applied to the cathode was 70 kV during this period, which produced an electric field of 350 V/cm in the TPC volume. In this section, we present results on the measurements of electron attenuation using these data.

8.1 Reconstruction

There are 491 966 triggered events during this run period. We use the LARSOFT software package v02_00_01 to reconstruct cosmic ray muon events. The automated reconstruction first converts the raw signal from each wire to a standard shape such as a Gaussian shape, and then finds hits and defines clusters. Three dimensional tracks are constructed from pairs of line-like clusters in each plane. There are 274 491 events with at least one reconstructed track (212 626 events with exactly one reconstructed track). Fig. 8 shows one example event after the full reconstruction chain.

In this analysis we only consider events with exactly one reconstructed track that has at least 5 reconstructed 3-dimensional trajectory points. We do not use events with multiple muon tracks

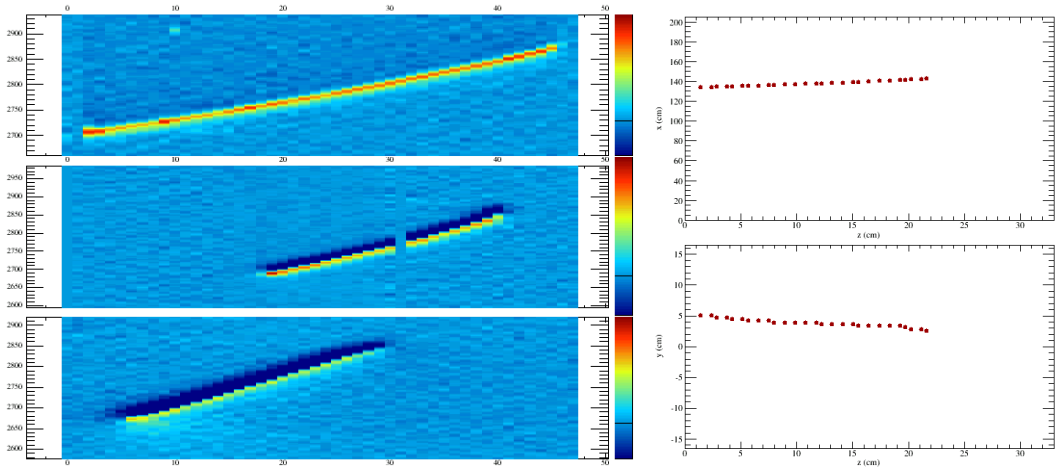

(a) Raw data (b) Reconstructed track

Figure 8: Run 293 Event 2225. (a) Drift time versus wire ID for raw wire signal from 3 wire planes. Red color represents high positive charge and blue color represents high negative charge. (b) Reconstructed track points in the x-z and y-z projections.

because we cannot determine the track start time, t_0, for each track. Fig. 9 shows the angular distributions of the reconstructed tracks. The track angle is determined by the reconstructed track start and track end assuming the track is a straight line. The θ angle is peaked around 60° and the ϕ angle is determined by the trigger counter locations. Fig. 10 shows the reconstructed track start point x, in the drift direction, versus the θ angle. $x = 0$ is near the wires. The muons normally enter the TPC in the middle, but they can be close to the wire planes and cathode.

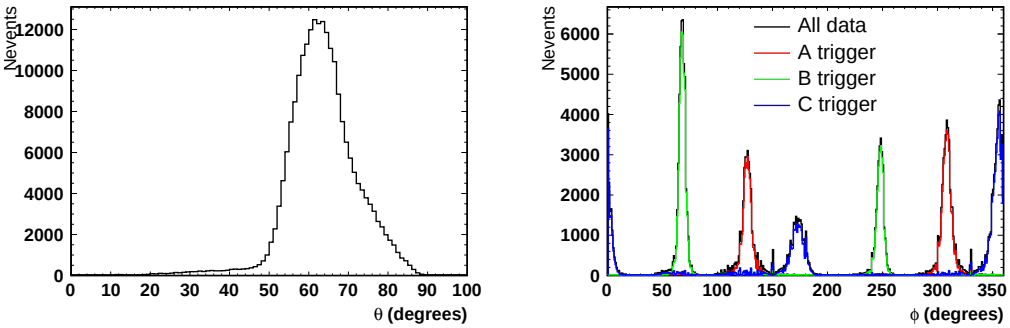

(a) Track θ (b) Track ϕ

Figure 9: Reconstructed track angles: (a) θ - with respect to the vertical direction; (b) ϕ, events taken with different triggers have distinct ϕ distributions. $x = 0$ is near the wires and $\theta = 0$ is at the zenith.

8.2 Electron Attenuation Measurement

We use clean muon tracks to measure electron attenuation in liquid argon. We first select events

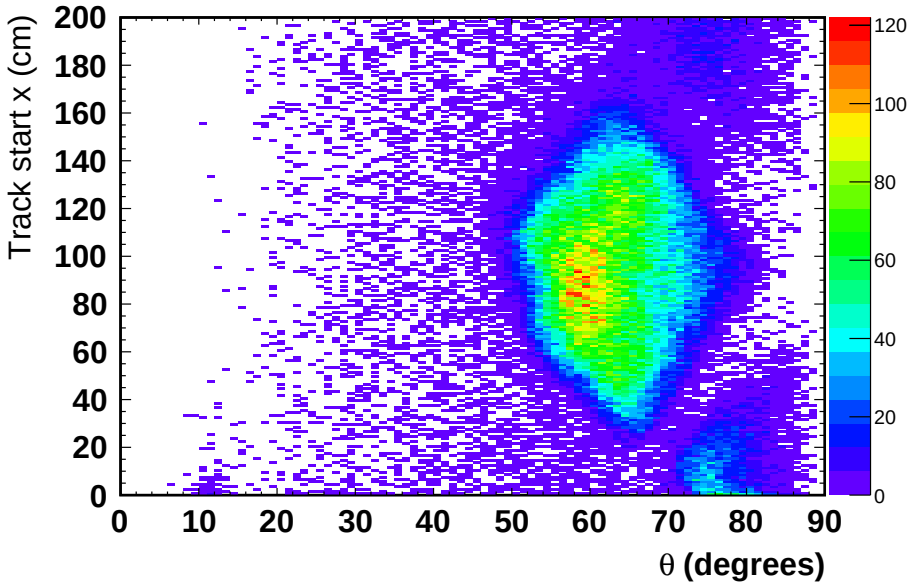

Figure 10: Reconstructed track start point in the drift direction (x) versus track angle (θ).

with well reconstructed and clean tracks:

1. the RMS distance of reconstructed space points with respect to a straight line determined by track start and end should be less then $\sqrt{40}$ mm;

2. the number of hits that are not associated with the reconstructed track should be less than 11;

3. track length is required to be greater than 15 cm;

4. track length $\times \cos\phi_{\text{track}}$, the projection along the collection plane trigger direction, is required to be greater than 10 cm;

5. θ_{track} is required to be tween 50° and 70°.

We then select all hits on the collection plane, except the first and last in time, associated with the tracks. We require only one hit on each wire. if there is one hit on each of three contiguous wires that has $dQ/dx > 2000$ ADC/cm, we do not use those three hits. This requirement is meant to remove delta rays.

For each selected hit, we look at raw wire signal for that hit in the region $[t-3\times\sigma, t+3\times\sigma]$, where t is the reconstructed hit time and σ is the reconstructed hit width. We first find the peak of the raw digits in ADC, we then sum all the digits above a threshold of 10% of the peak to get the charge of the hit. By using raw wire signal we remove uncertainties introduced by signal shaping in the hit reconstruction. We then divide the hit charge by the track pitch, which is defined as the wire pitch over dot product of the track direction and the direction normal to the wire direction in the wire plane, to get dQ/dx for the hit.

Figure 11a shows hit dQ/dx versus electron drift time distribution using data taken in a 2-hour window. Fig. 11b shows dQ/dx distribution for hits with drift time betwen 456 and 482 μs (shaded area in Fig. 11a). We fit a Landau convoluted with Gaussian function to the dQ/dx distribution. An example fit is shown in Fig. 11b. Fig. 11c shows the most probable value (MPV) from the Landau fit as a function of drift time. The signal decreases as drift time increases as expected. We fit an exponential function to the data points:

$$dQ/dx = e^{-at_d+b}, \tag{8.1}$$

where t_d is the drift time and a is the attenuation constant. Fig. 12 shows $dQ/dx_0 = dQ/dx(t = 0) = e^b$ as a function of time and it is relatively flat. The attenuation constant is corrected for electron diffusion, which is described in Appendix **A**.

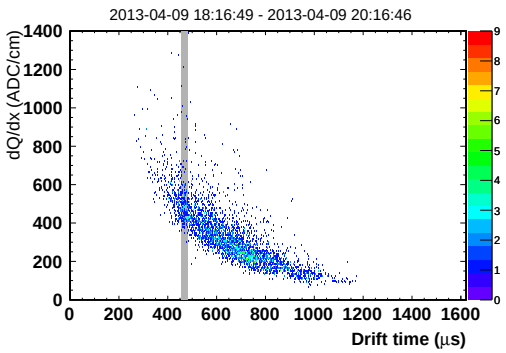

(a) dQ/dx versus drift time

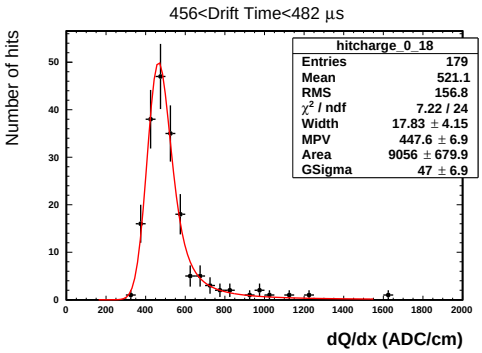

(b) dQ/dx for hits with drift time between 456 and 482 μs

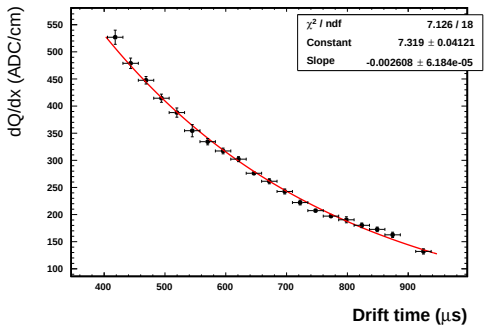

(c) dQ/dx from Landau fit versus drift time - 1D

Figure 11: dQ/dx distributions of hits using data taken in a 2-hour window. (a) Scatter plot of dQ/dx as a function of electron drift time; (b) dQ/dx distribution for hits with drift time between 456 and 482 μs; (c) dQ/dx from Landau fit as a function of drift time.

LAPD reported the measurement of electron attenuation using purity monitors [1]. The result was presented as Q_A/Q_C as a function of time, where Q_A/Q_C represents the fraction of electrons generated at the purity monitor cathode that arrive at the anode. It is determined by the electron drift time (t_d) and electron lifetime (τ) or attenuation constant (a):

$$Q_A/Q_C = e^{-t_d/\tau} = e^{-at_d}. \tag{8.2}$$

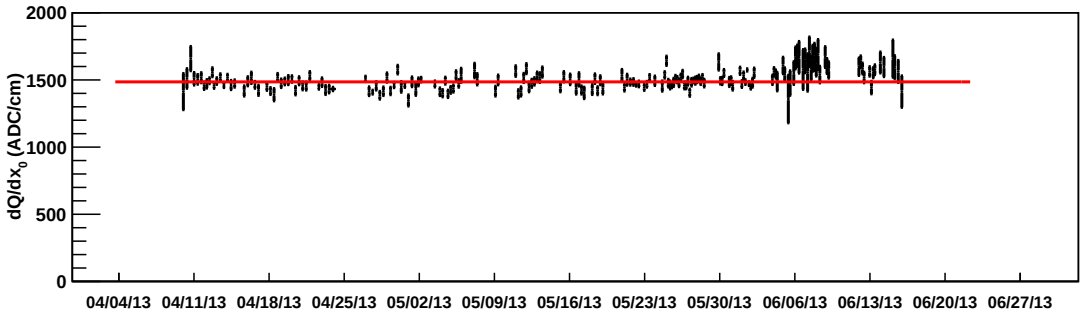

Figure 12: dQ/dx_0 as a function of time.

In order to compare the measurement using TPC data with the measurement using purity monitors, we calculate the equivalent Q_A/Q_C using the attenuation constant measured by the TPC data and $t_d = 0.38$ ms, which is the electron drift time from the cathode to the anode grid in the purity monitor. Fig. 13 shows the comparison between Q_A/Q_C measured by the purity monitors and the calculated Q_A/Q_C using attenuation constant measured using the TPC data. The statistical errors from the original Landau fits are propagated through the attenuation fits to Fig. 13, and are smaller than the red points.

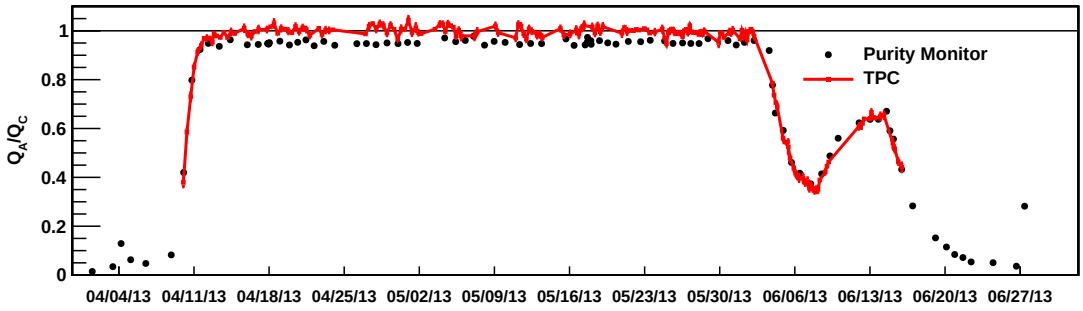

Figure 13: Comparison between Q_A/Q_C measured by the purity monitors and the calculated Q_A/Q_C using attenuation constant measured using the TPC data.

The attenuation measurement using the TPC is in a good agreement with the measurement using purity monitors when the attenuation is greater than 10% in the purity monitor. When the liquid argon is very purity, that is attenuation less than 10%, there is a noticeable difference between the two measurements most likely caused by systematic effects in both techniques.

9. Conclusions

A ratio $S/N = 50.5/1.7 \sim 30$ was measured for the wires in the collection plane with discrete CMOS electronics in the LAPD/LongBo TPC, which has a wire spacing of 4.7 mm. For these data the TPC was operated with a drift field of 350 V/cm. The measured S/N ratio for the ASIC

channels was 1.44 times larger than that measured for the discrete channels for the ASIC shaping time of 2.0 μs and a gain setting of 25 mV/fC.

A. Correction for Diffusion

While we were measuring electron attenuation using cosmic ray muons, we observed an electron "gain" when the liquid argon was very pure, i.e. the signal was higher at longer drift time, which suggests not only the electron absorption is negligible, but also the signal is getting bigger as the electrons travel toward the wire planes. We have investigated many systematic effects that may cause this "negative lifetime" artifact. The most likely explanation is electron diffusion.

We simulate a sample of 10 000 single muons at a fixed momentum of 6 GeV/c. The vertex x (drift direction) is uniformly distributed between 50 and 150 cm while y = z = 0 cm are on the edge of the TPC. The θ angle is uniformly distributed between 50° and 70° while the ϕ angle is fixed at 0°. GEANT4 is used to simulate particle propagation in the liquid argon. The electron drifting and signal collection is simulated using LARSOFT taking into account of recombination, attenuation and diffusion.

We then run the same reconstruction and analysis chain, described in Section 8, on the simulated events. Fig. 14a shows dQ/dx as a function of drift time when we use the default diffusion simulation. The diffusion is assumed to be Gaussian in the simulation with these widths:

$$\sigma_L = \sqrt{2t_d D_L} \tag{A.1}$$

$$\sigma_T = \sqrt{2t_d D_T} \tag{A.2}$$

where t_d is the electron drift time, D_L and D_T are the longitudinal and transverse diffusion constants:

$$D_L = 6.2 \times 10^{-9} \mathrm{cm}^2/\mathrm{ns} \tag{A.3}$$

$$D_T = 16.3 \times 10^{-9} \mathrm{cm}^2/\mathrm{ns} \tag{A.4}$$

The longitudinal diffusion is in the electron drift direction and the transverse diffusion in the direction normal to the drift direction.

We fit an exponential function to the dQ/dx distribution and the fitted slope is clearly positive. Fig. 14b shows the similar distribution with both longitudinal and transverse diffusion turned off ($D_L = D_T = 0$). The fitted slope is consistent with being zero. We take the difference between the two slopes and use it to correct data for diffusion effect. The difference (positive) is added to the measured attenuation constant. We also simulated events with only transverse diffusion ($D_L = 0, D_T = default$) and with only longitudinal diffusion ($D_T = 0, D_L = default$) and the positive slope is caused by the transverse diffusion. The transverse diffusion smears the electrons between neighboring wires. We also verify in the simulation more electrons arrive at the wires at a longer drift time if we turn on the diffusion.

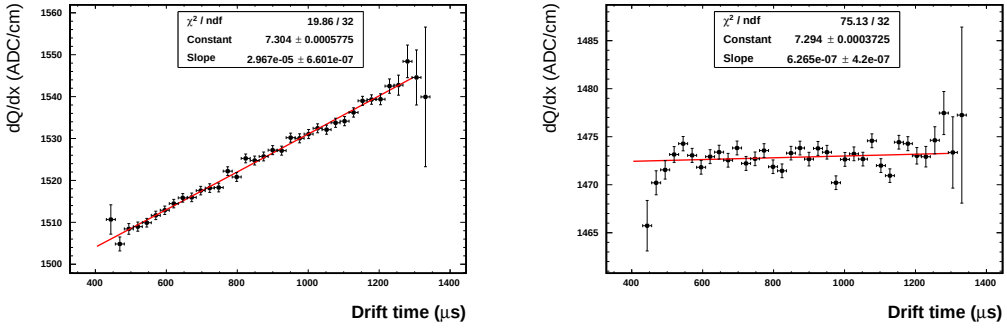

(a) Default diffusion (b) No diffusion

Figure 14: Simulated dQ/dx vs drift time with (a) Default diffusion; (b) No diffusion.

Acknowledgments

References

[1] M. Adamowski, B. Carls, E. Dvorak, A. Hahn, W. Jaskierny, C. Johnson, H. Jostlein and C. Kendziora *et al.*, JINST **9**, P07005 (2014).

[2] C. Anderson, M. Antonello, B. Baller, T. Bolton, C. Bromberg, F. Cavanna, E. Church and D. Edmunds *et al.*, JINST **7**, P10019 (2012).

[3] Glassman High Voltage Inc., PO Box 317, 124 West Main Street, High Bridge, NJ 08829-0317, U.S.A. www.glassmanhv.com